JOURNAL OF APPLIED ELECTROCHEMISTRY **28** (1998) 797–801

Electrodeposition of silver from nitrate solution: Part II. Mechanism of the effect of phosphate ions

K. I. POPOV, M. G. PAVLOVIC, B. N. GRGUR

Faculty of Technology and Metallurgy, University of Belgrade, Yugoslavia

A. T. DIMITROV, S. HADZI JORDANOV

Faculty of Technology and Metallurgy, University "St Cyril & Methodius", Skopje, Macedonia

Received 11 November 1996; revised 4 July 1997

The mechanism of compact Ag-film formation by electrolysis from nitrate solution with addition of small amounts of phosphate ions is elucidated. It is shown that the phosphate ions exert their effect by lowering the exchange current density. Consequently, the radii of nucleation exclusion zones also diminishes, thus producing conditions stimulating electrodeposition of continuous thin Ag-film.

Keywords: *electrodeposition*, *nitrate solution*, *phosphate ion addition*, *silver*

List of symbols

C	concentration of adatoms at the electrode surface
C_0	equilibrium concentration of adatoms
E	cell voltage
f	numerical factor accounting for deviation of geometry
J	nucleation rate
j	current density
j_0	exchange current density
α	transfer coefficient
η	overpotential
η_c	critical overpotential for nucleation to occur
η_{cr}	crystallization overpotential
ρ	radius of nucleus hemispherical drop

1. Introduction

In our previous paper [1] it was shown that the addition of phosphate ions, together with stirring of the nitrate electrolyte for silver electrorefining, produces conditions favourable for compact silver deposition. Normally, from clean nitrate solution and without stirring compact Ag is not deposited.

The goal of this paper is to offer explanation for the measured effect of phosphate ions to the morphology of silver deposits.

2. Experimental details

Silver was deposited onto Ag and Pt substrates from aqueous solutions containing 0.5 M $AgNO_3$ + 100 g dm^{-3} $NaNO_3$ and 0.5 M $AgNO_3$ + 100 g dm^{-3} $NaNO_3$ + 6 g dm^{-3} H_3PO_4, all of analytical grade and doubly-distilled water. Galvanostatic and potentiostatic plating conditions were applied and the cell was of an open type. The counter and the reference electrode were of analytical-grade pure silver. The polarization curves were taken potentiostatically on to silver substrates, while the thin Ag-film was deposited on to a Pt substrate. The Ag-deposit morphology was determined by use of a SEM (Joel T20 type).

The a.c.-impedance measurements were performed in a glass cell, thermostated at 298 ± 0.1 K and in a purified argon atmosphere. The working electrode was a Ag wire (0.5 cm^2), the counter electrode a Pt sheet (2 cm^2) and a $Hg/Hg_2Cl_2/KCl$ (satd) (SCE) electrode in an agar–agar–KNO_3 double junction bridge was used as a reference electrode.

The a.c.-impedance spectra were obtained with a PAR (M273) potentiostat, a lock-in amplifier (M5301) and an IBM (PS2/M30) compatible computer, interfaced with a GPIB card. The frequency was scanned from high to low values, for example, from 30 kHz to 50 mHz, with an amplitude to ±3 mV only, due to the fact that dissipation of measured values occurred when higher amplitudes were applied.

3. Results and discussion

In Fig. 1 polarization curves taken in electrolytes containing zero or the indicated concentration of phosphate ions are shown. It is obvious that, in the presence of phosphate ions, any value of c.d. can be achieved at lower overpotentials, indicating at first glance the possible catalysis of the deposition process, and a rise of the exchange current-density, respectively. In order to confirm this idea, the exchange current-density was determined.

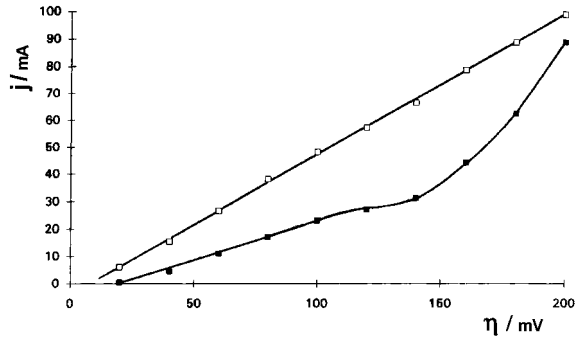

Fig. 1. Polarization curves for a silver electrode (0.5 cm^2) in: (■) 0.5 M $AgNO_3$ in 100 g dm^{-3} $NaNO_3$ and (□) + 6 g dm^{-3} H_3PO_4.

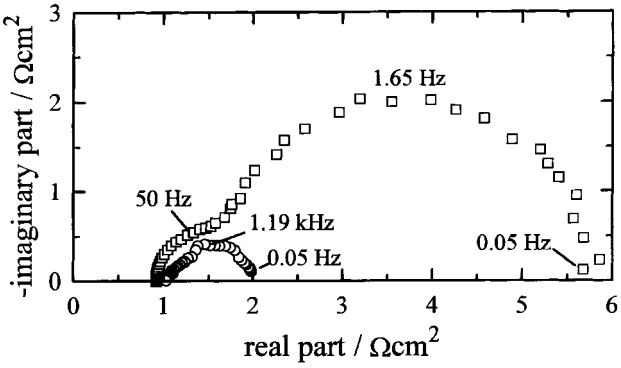

Fig. 2. Impedance spectra for Ag electrodeposition in a solution of 0.5 M $AgNO_3$ (○) and 0.5 M $AgNO_3$ with the addition 6.0 g dm^{-3} H_3PO_4 (□).

In Fig. 2 the a.c.-impedance spectra in the absence and presence of PO_4^{3-} anions at $\eta = 0$ (0.543 V and 0.48 V vs SCE, respectively) are shown.

According to the Schmidt *et al.* [2] the impedance Z_s of the Ag electrocrystallization process corresponds to a Nernst diffusion impedance in series with a lateral transport diffusion impedance in a parallel with an adatom pseudo-capacitance. Approaching conditions when frequency tends to zero, Z_s consists only of the resistance parameter R_0 which is connected with the current density as follows:

$$j = \frac{RT}{zFR_0}\exp\left(\frac{-F\eta}{RT}\right) \tag{1}$$

where, at $\eta = 0$, j_{ss} is approximately equal to the exchange current density, that is,

$$j_{ss}(\eta = 0) \approx j_0 \approx \frac{RT}{zFR_0} \tag{2}$$

Hence, R_0 measured in the 0.5 M $AgNO_3$ is 1 $\Omega\,cm^2$ and in the presence of PO_4^{3-}, 5 $\Omega\,cm^2$ or $j_0 \approx$ 26 mA cm^{-2} and 5 mA cm^{-2}, respectively (Fig. 2).

These differences in R_0 and j_0 values, respectively, are high enough to be attributed to the formation of Ag^+ and PO_4^{3-} complexes because the concentration of PO_4^{3-} was ten times lower (0.06 M) than that of the Ag^+ ions. Probably the effect of phosphate anion is through its adsorption on the electrode surface at high negative potentials. Thus, the process of silver electrocrystallization takes place through formation of an intermediate adsorption complex, probably according to the following mechanism:

$$Ag^+ + \left(PO_4^{3-}\right)_{ads} \longrightarrow \left(AgPO_4^{2-}\right)_{ads} \tag{3}$$

$$\left(AgPO_4^{2-}\right)_{ads} + e^- \longrightarrow Ag + \left(PO_4^{3-}\right)_{ads} \tag{4}$$

The shift in the reversible potential by −60 mV in the presence of phosphate ions and the high capacitance of the second semicircle (18 mF) is an indication that the proposed mechanism is valid. Accordingly, the shape of the polarization curve in the presence of the phosphate ions is explained only by the change of the surface state.

In Fig. 3 a comparison is shown of the morphology of Ag grains deposited onto Pt substrate from nitrate solutions without and with PO_4^{3-} ion addition. The double current pulse technique was applied. In our previous paper [1] it was shown that the deposition of silver on both substrates, Pt and Ag, starts with 3D nucleation. This type of nucleation was more pronounced on Pt and this is the reason why the deposition in this work was made onto this substrate. From Fig. 3 it can be seen that in the presence of phosphate ions the deposited silver is distributed

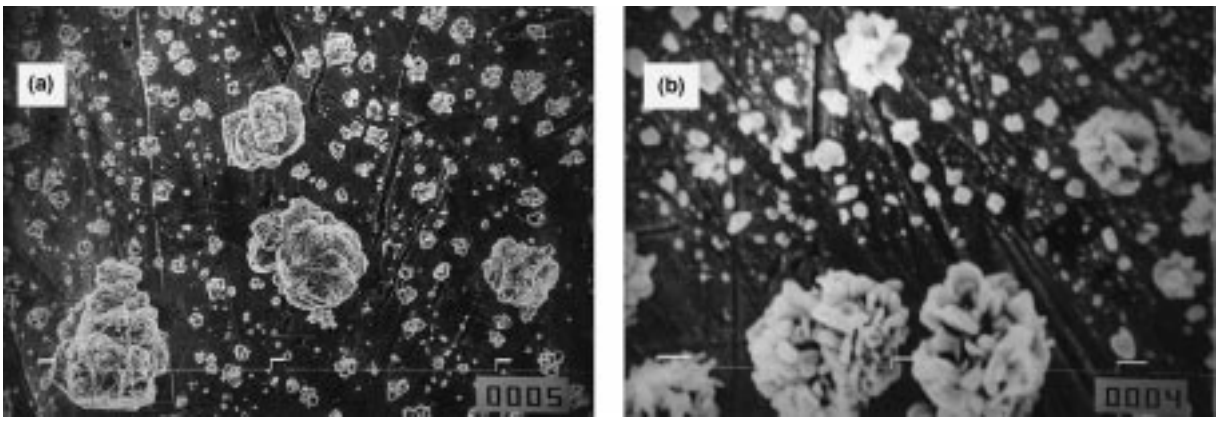

Fig. 3. Silver electrodeposits obtained onto a stationary platinum wire electrodes with a double galvanostatic current pulse: $\tau_1 = 100$ s, $I_1 = 1$ mA; $\tau_2 = 2$ s, $I_2 = 35$ mA (a) 0.5 M $AgNO_3$ + 100 g dm^{-3} $NaNO_3$ Magnification × 350; (b) 0.5 M $AgNO_3$ + 100 g dm^{-3} $NaNO_3$ + 6 g dm^{-3} H_3PO_4 Magnification × 3500.

among a fairly large number of particles, having remarkably larger total surface area, and leading to significantly higher current intensity when other conditions are the same. In this case the galvanostatic technique was applied to make the quantity of deposited metal easier to control.

Metal electrodeposition on inert electrodes begins by the formation of separate centres growing further until a continuous or disperse deposit is produced. Although the kinetics of electrolytic nucleation and subsequent growth have been subject of extensive studies, little attention has been paid to the screening action of the growing nuclei. The nature of this phenomenon should be made clear by the following arguments: once a nucleus of the depositing metal is formed, the passing current causes a local deformation of the electric field in the vicinity of the growing centre. As a result, an ohmic potential drop arises along the nucleus–anode direction. Considering the steep dependence of the nucleation rate on the overpotential, it is expected that new nuclei will form only outside a certain spatial region around the initial nucleus where the potential difference between the cathode and the electrolyte surpasses some critical value η_c [3].

In a previous paper [1] Equation 1 was given for the dependence of the radius of the screening zone on the E and η_c (E_k) values. At constant η_c the increase of E leads to the decrease of the radius of screening zone. The same appears if η_c decreases at constant E.

The crystallization overpotential, expressed as

$$\eta_{cr} = \frac{RT}{zF} \ln \frac{C}{C_0} \tag{5}$$

clearly shows the importance of the supersaturation ratio C/C_0 for the crystallization process. It allows to estimate how much the equilibrium coexistence of adatoms and crystals has been surpassed to make possible formation of new crystal nuclei.

It is known that the overpotential measured in the moment of nucleation is a sum of crystallization and charge transfer overpotentials (if other kinds of polarization can be neglected). The critical and crystallization overpotential are equal to each other only in the case when the charge transfer overpotential can be neglected ($j_0 \to \infty$).

The polarization curve of the overall reaction is expressed by the equation of the transfer reaction modified with respect to crystallization process:

$$j = j_0 \left\{ \frac{C}{C_0} \exp\left(\frac{\alpha z F}{RT}\eta\right) - \exp\left[\frac{-(1-\alpha)zF}{RT}\eta\right] \right\} \tag{6}$$

To calculate polarization curves from Equation 6 it is necessary to determine the value of the supersaturation ratio C/C_0. The lower limit for the cathodic process is equal to unity in which case Equation 6 becomes identical with equation of the charge transfer reaction. For the upper limit it can be assumed that C/C_0 reaches values up to 10, being larger than 4–7 as reported by Pangarov *et al.* [4–6].

During the cathodic process at low j/j_0 the crystallization overpotential is considerably high, but with increasing j/j_0, however, it rapidly decreases [7]. Hence, for $j_0 \to 0$, $r \to 0$.

It was experimentally demonstrated that number of nuclei deposited electrolytically on to inert electrodes increases linearly with time, after a period of induction. After a sufficient time it reaches a saturation value that is independent of time. The saturation density increases with the applied overpotential and is strongly dependent on the concentration of the electrolyte and the state of electrode surface [8–10].

Kaischev and Mutaftchiev [11] explained the phenomenon of saturation on the basis of energetic inhomogenity of the substrate surface. They assumed that the active centres have different activity, or different critical overpotential, respectively. Nuclei can be formed only on centres with critical overpotential lower than or equal to the applied potential. The higher the overpotential applied, the greater the number of (weaker) active sites taking part in the nucleation process, and hence the greater nucleus saturation density. The formation and growth of nuclei is necessarily followed by the formation and growth of nucleation exclusion zones. After some time the zones overlap to cover the substrate surface exposed for nucleation, thus terminating the nucleation process.

The simultaneous action of both active centres and nucleation exclusive zones is to be taken into consideration in discussing the dependence of the number of nuclei on time. In the limiting case for active centres, when screening zones do not form, the nucleus saturation density is exactly equal to the integral number of active centres. In the limiting case for nucleation exclusive zones only, the nucleus saturation density is directly proportional to the nucleation rate and inversely to the zone growth rate [10]. It is obvious that nucleus saturation density is larger in the former than in the latter case, because of the deactivation of active centres by overlapping nucleation exclusive zones.

The classical expression for the steady state nucleation rate J is given by [12, 13]:

$$J = K_1 \exp\left(-\frac{K_2}{\eta^2}\right) \tag{7}$$

where K_1 and K_2 are practically overpotential-independent constants. Equation 7 is valid for a number of systems regardless of the exchange current density value for deposition process [14–18]. At one and the same deposition current density, j, decreasing j_0 leads to the increasing nucleation rate and the decreasing nucleation exclusion zones radii. Hence, for $j/j_0 \to 0$ the limiting case for nucleation exclusion zones can be expected, and for $j/j_0 \to \infty$ the limiting case for active centres.

The nucleus saturation density, that is, the exchange current density, strongly affects the morphology of metal deposits. At high exchange current densities the radii of screening zones are

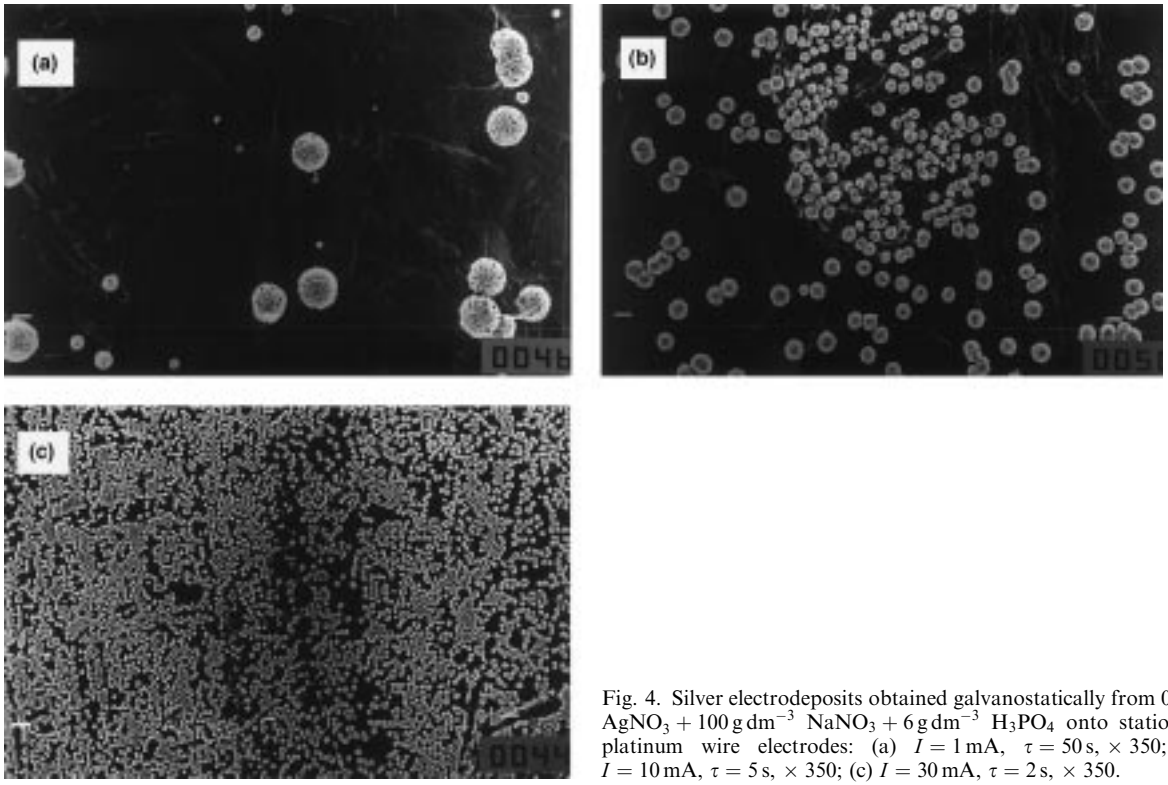

Fig. 4. Silver electrodeposits obtained galvanostatically from 0.5 M $AgNO_3 + 100\,g\,dm^{-3}$ $NaNO_3 + 6\,g\,dm^{-3}$ H_3PO_4 onto stationary platinum wire electrodes: (a) $I = 1\,mA$, $\tau = 50\,s$, $\times$ 350; (b) $I = 10\,mA$, $\tau = 5\,s$, $\times$ 350; (c) $I = 30\,mA$, $\tau = 2\,s$, $\times$ 350.

larger and nucleus saturation density is low. This permits the formation of large, well defined crystal grains and granular growth of deposit. At low exchange current densities the screening zones radii are low, or equal to zero, the nucleation rate is large and thin surface film can be formed easily.

In Figs 4 and 5 silver deposits formed from PO_4^{3-}-ion containing electrolyte on to Pt substrate with galvanostatic current pulses are shown. Significant morphology differences are visible between these and the deposits formed from solutions free of phosphate ions. The compared grains differ both in their mutual distribution and in their shape. At a current density of $30\,mA\,cm^{-2}$ (i.e. the optimal film deposition conditions, as determined in our previous study [1]), almost complete surface coverage was achieved even

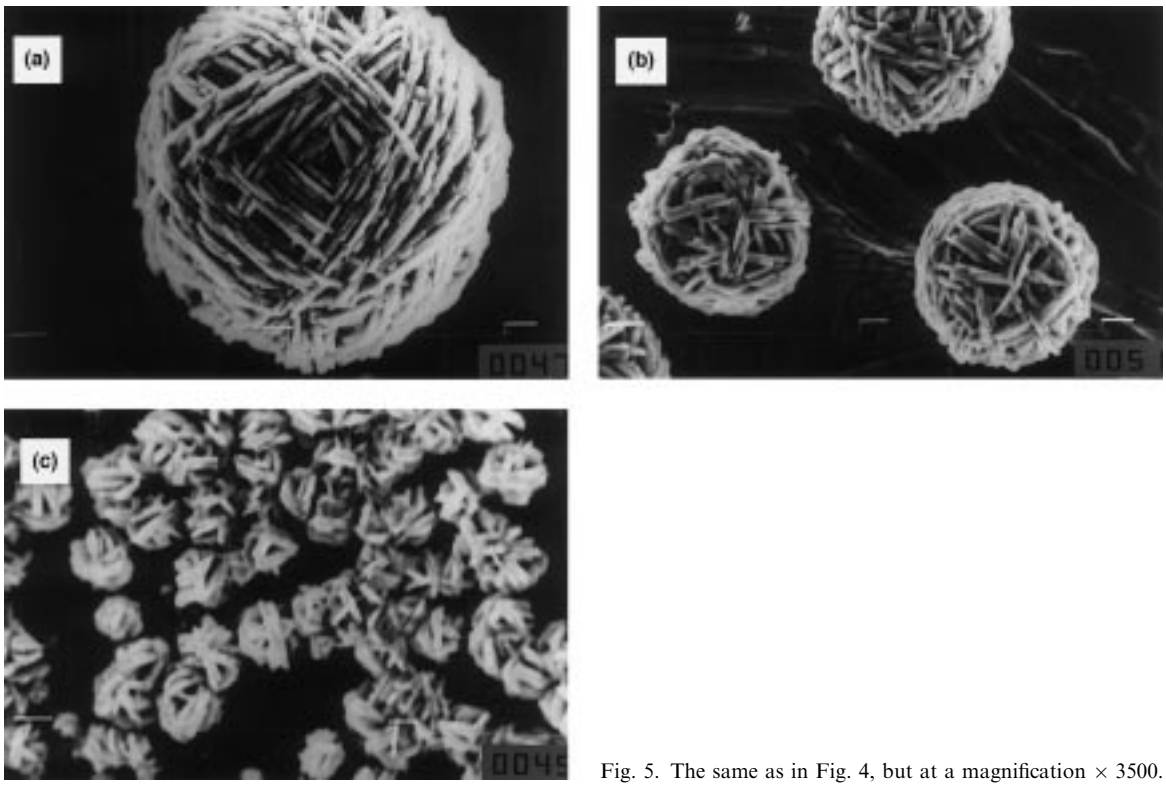

Fig. 5. The same as in Fig. 4, but at a magnification $\times$ 3500.

with a charge quantity of $2\,mA\,h\,cm^{-2}$. For comparison, in phosphate-free nitrate solutions, compact Ag film was not deposited even after $100\,mA\,h\,cm^{-2}$ were passed through the cell [1]. This is probably due to the possibility of further nucleation taking place immediately next to the already existing nuclei, as a result of smaller values of the radii of the nucleation exclusion zones. Additionally, the structure of the deposits described in our previous paper [1] was with no doubt caused by the difference in shapes of grain deposited in the presence of phosphates as compared with the previously produced ones in the absence of phosphates.

At the present time it is not possible to explain why such changes occur.

4. Conclusions

The mechanism of the effect of addition of phosphate ions on the morphology of electrolytic silver deposits generated from stirred nitrate solutions is elucidated.

It is shown that addition of phosphate anions lowers the exchange current density sufficiently for the nucleation saturation density to acquire values when the formation of compact silver deposits is possible. The shape and the size of the Ag-grains are also changed by the presence of phosphate ions so that thick silver layers having a fibrous structure are produced.

Acknowledgment

We thank Professor B. E. Conway, University of Ottawa, ON, Canada for careful inspection of the manuscript and useful suggestions and Ms E. Stoilkovic for producing the semicrographs.

References

[1] A. Dimitrov, S. Hadzi Jordanov, K. I. Popov, M. G. Pavlovic and V. Radmilovic, *J. Appl. Electrochem.* **28** (1998) 791–796.
[2] E. Schmidt, J. Hitzig, J. Titz, K. Juther and W. J. Lorenz, *Electrochim. Acta* **31** (1986) 1044.
[3] I. Markov, A. Boynov and S. Toschev, *ibid.* **18** (1973) 377.
[4] N. A. Pangarov and S. D. Vitkova, *ibid.* **11** (1966) 1719.
[5] N. A. Pangarov and V. Velinov, *ibid.* **11** (1966) 1793.
[6] N. A. Pangarov, S. D. Vitkova and J. Uzunova, *ibid.* **11** (1966) 1747.
[7] V. Klapka, *Collection Czechoslov. Chem. Comun.* **35** (1970) 899.
[8] S. Toshev and I. Markov, *Ber. Buunseges. Phys. Chem.* **73** (1969) 184.
[9] A. Scheludko and M. Todorova, *Comn. Bulg. Acad. Sci. (Phys)* **3** (1952) 61.
[10] I. Markov, *Thin Solid Films* **35** (1976) 11.
[11] R. Kaischew and B. Mutaftchiew, *Electrochim. Acta* **10** (1965) 643.
[12] R. Becker and W. Döring, *Ann. Phys. (Leipzig)* **24** (1935) 719.
[13] G. Tohmfor and M. Volmer, *ibid.* **B33** (1938) 109.
[14] R. Kaischew and B. Mutaftchiew, *Z. Phys. Chem.* **204** (1955) 334.
[15] B. Mutaftschiew and R. Kaischew, *Izv. BAN* **5** (1955) 77.
[16] R. Kaischew and I. Gutzow, *Electrochim. Acta* **9** (1964) 1047.
[17] A. Scheludko and G. Bliznakov, *Izv. BAN* **2** (11951) 227.
[18] I. Gutzow, *Izv. Inst. Fiz. Chim. Bulgar. Acad. Nauk* **4** (1964) 69.